საქართველოს მეცნიერებათა ეროვნული აკადემიის მოამბე, ტ. 6, №1, 2012
BULLETIN OF THE GEORGIAN NATIONAL ACADEMY OF SCIENCES, vol. 6, no. 1, 2012

Mechanics

Characteristics of the Solution of the Consistently Linearized Eigenproblem for Lateral Torsional Buckling

Mehdi Aminbaghai* and Herbert A. Mang*

* *Institute for Mechanics of Materials and Structures, Vienna University of Technology, Vienna, Austria*

ABSTRACT. The consistently linearized eigenproblem has proved to be a powerful mathematical tool for classification of buckling, based on the percentage bending energy of the total strain energy. Of particular interest are prebuckling states with a constant percentage strain energy. The two limiting cases of such states are membrane stress states and states of pure bending. Buckling at pure bending, referred to as lateral torsional buckling, is the topic of this work. The transfer matrix method is used to derive a secant stiffness matrix in analytical form. Formulation of the consistently linearized eigenproblem by means of this matrix yields the same solution as would be obtained by a formulation based on the tangent stiffness matrix which is an essential ingredient of nonlinear Finite Element Analysis. This remarkable finding permits analytical verification of hypothesized subsidiary conditions for lateral torsional buckling. *© 2012 Bull. Georg. Natl. Acad. Sci.*

Key words: *consistently linearized eigenproblem, lateral torsional buckling, transfer matrix method.*

1. Introduction

Recently, Mang et al. [1] reported on Finite Element Analysis (FEA) of elastic structures at special prebuckling states which were defined as states with a constant percentage bending energy of the strain energy in the prebuckling regime. This regime is characterized by a proportional increase of the reference load. One of the two limiting cases of such states is a membrane stress state. This case was treated in detail in a paper by Mang and Höfinger [2].

The present work deals with the second limiting case, which is buckling at pure bending, referred to as lateral torsional buckling. The purpose of the paper is to prove subsidiary conditions for this special case, in the context of the Finite Element Method (FEM), hypothesized in [1] on the basis of the consistently linearized eigenproblem which was introduced by Helnwein [3]. In order to free the proof from discretization errors, typical for results obtained by the Finite Element Method (FEM), these conditions are verified through numerical evaluation of an analytical solution obtained by means of the transfer matrix method [4].

The paper is organized as follows: In Chapter 2, the differential equation for the rotation of the cross-section of a beam subjected to pure, skew bending about the axis of the beam is presented. Chapter 3 is devoted to the analytical solution of this differential equation, followed by the formation of the transfer matrix. The mathematical expression for the rotation depends on a dimensionless load factor by which the reference bending moment is multiplied, and on the axial coordinate. Buckling at pure bending requires a constant reference bending moment. In Chapter 4, the secant stiffness matrix is derived analytically with the help of the transfer matrix method. In Chapter 5, the formulation of the consistently linearized eigenproblem on the basis of the secant stiffness matrix is shown to give the same result as would be obtained by means of the tangent stiffness matrix. Chapter 6 contains the numerical investigation. Conclusions from this work are drawn in Chapter 7.

2. Differential Equation

Fig. 1 shows a fork-supported beam of length l with a constant, doubly symmetric cross-section. At its ends, the beam is subjected to bending moments

$$M_{y,b} = M_{y,a} = M_y = \lambda \bar{M}_y, \tag{1}$$

$$M_{z,b} = M_{z,a} = M_z = \lambda \bar{M}_z, \tag{2}$$

where $\bar{M}_y$ and $\bar{M}_z$ are reference quantities and λ is a dimensionless load factor. Hence, the prebuckling state is one of pure bending.

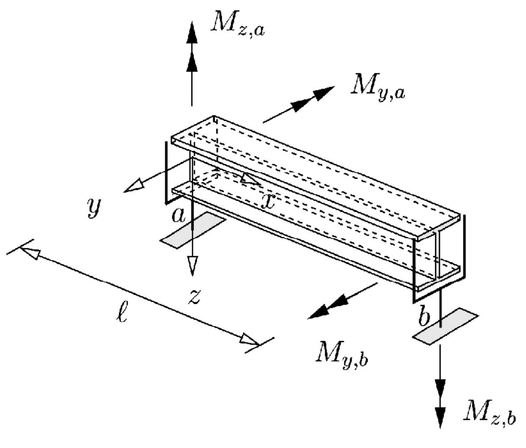

Fig. 1. Fork-supported beam subjected to pure, skew bending.

The differential equation for the rotation ϑ of the cross-section of the beam about the x-axis (Fig. 2) follows from [5], considering (1) and (2), as

$$EI_\omega \vartheta'''' - GI_T \vartheta'' - \frac{1}{EI_y}\left(\frac{I_y}{I_z}\bar{M}_y^2 + \bar{M}_z^2\right)\lambda^2\vartheta = \frac{\bar{M}_y \bar{M}_z}{EI_y}\left(1 - \frac{I_y}{I_z}\right)\lambda^2, \tag{3}$$

where I_y and I_z are the principal moments of inertia, I_T is St. Venant's torsion constant, I_ω is the warping constant, E is Young's modulus, and G is the shear modulus.

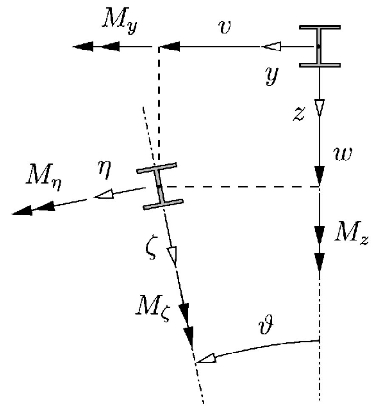

Fig. 2. Cross-section of the beam in the undeformed and the deformed position of the structure.

Eq. (3) is based on the assumption of small prebuckling rotations for which

$$\sin\vartheta \approx \vartheta, \quad \cos\vartheta \approx 1, \tag{4}$$

resulting in

$$M_\eta = M_y + M_z\vartheta, \quad M_\zeta = M_z - M_y\vartheta. \tag{5}$$

If $\bar{M}_y = 0$ or $\bar{M}_z = 0$, or $I_z = I_y$, (3) becomes a homogeneous differential equation, representing an eigenproblem. The smallest eigenvalue, $\lambda = \lambda_S$, defines the buckling moment. The corresponding eigenfunction, $\hat{\vartheta}(x)$, permits determination of the buckling mode. If $\bar{M}_y \neq 0$ and $\bar{M}_z \neq 0$, and $I_z \neq I_y$, $\vartheta(x,\lambda)$, $0 < x < l$, tends to infinity as λ approaches λ_S, which is in contradiction to (4). However, this well-known deficiency of second-order theory is no obstacle for reaching the goals of this work.

Introducing the abbreviations

$$b = \frac{GI_T}{EI_\omega},$$

$$c(\lambda) = \frac{GI_T}{E^2 I_z I_\omega}\left(\frac{I_y}{I_z}\bar{M}_y^2 + \bar{M}_z^2\right)\lambda^2,$$

$$d(\lambda) = \frac{\bar{M}_y \bar{M}_z}{EI_y}\left(1 - \frac{I_y}{I_z}\right)\lambda^2, \tag{6}$$

Eq. 3 is rewritten as

$$\vartheta''''(x,\lambda) - b\vartheta''(x,\lambda) - c(\lambda)\vartheta(x,\lambda) = d(\lambda). \tag{7}$$

3. Solution of the Differential Equation and Formation of the Transfer Matrix

According to Schneider and Rubin [6], the solution of the inhomogeneous, linear, ordinary differential equation of fourth order in ϑ (7) is obtained as

$$\vartheta(x,\lambda) = \vartheta_a(\lambda)\mu_1(x,\lambda) + \vartheta_a'(\lambda)\mu_2(x,\lambda) + \vartheta_a''(\lambda)\mu_3(x,\lambda) + \vartheta_a'''(\lambda)\mu_4(x,\lambda) + d(\lambda)\mu_5(x,\lambda), \quad \lambda > 0, \tag{8}$$

where

$$\mu_1(x,\lambda) = \frac{f^2(\lambda)\cosh(f(\lambda)x) + g^2(\lambda)\cos(g(\lambda)x)}{2\sqrt{r(\lambda)}}, \tag{9}$$

$$\mu_2(x,\lambda) = \frac{f(\lambda)\sinh(f(\lambda)x) + g(\lambda)\sin(g(\lambda)x)}{2\sqrt{r(\lambda)}}, \tag{10}$$

$$\mu_3(x,\lambda) = \frac{\cosh(f(\lambda)x) - \cos(g(\lambda)x)}{2\sqrt{r(\lambda)}}, \tag{11}$$

$$\mu_4(x,\lambda) = \frac{\dfrac{\sinh(f(\lambda)x)}{f(\lambda)} - \dfrac{\sin(g(\lambda)x)}{g(\lambda)}}{2\sqrt{r(\lambda)}}, \tag{12}$$

$$\mu_5(x,\lambda) = \frac{1}{c(\lambda)}\left(\mu_1(x,\lambda) - 1 - b\mu_3(x,\lambda)\right), \tag{13}$$

with

$$r(\lambda) = \frac{1}{4}b^2 + c(\lambda), \tag{14}$$

$$f(\lambda) = \sqrt{\frac{b}{2} + \sqrt{r(\lambda)}}, \tag{15}$$

$$g(\lambda) = \sqrt{-\frac{b}{2} + \sqrt{r(\lambda)}}. \tag{16}$$

Formation of the transfer matrix begins with expressing the vector $\boldsymbol{\vartheta}_x$, the transpose of which is defined as

$$\boldsymbol{\vartheta}_x^T = \lfloor \vartheta(x,\lambda), \vartheta'(x,\lambda), \vartheta''(x,\lambda), \vartheta'''(x,\lambda) | 1 \rfloor, \tag{17}$$

in terms of the vector $\boldsymbol{\vartheta}_a = \boldsymbol{\vartheta}_x(x=0)$, the transpose of which is given as

$$\boldsymbol{\vartheta}_a^T = \lfloor \vartheta_a(\lambda),\ \vartheta_a'(\lambda),\ \vartheta_a''(\lambda),\ \vartheta_a'''(\lambda) \mid 1 \rfloor. \tag{18}$$

The purpose of the last coefficient in (17) and (18) is to render the matrix $\boldsymbol{F}_{xa}^*$ in the relation

$$\boldsymbol{\vartheta}_x = \boldsymbol{F}_{xa}^* \cdot \boldsymbol{\vartheta}_a \tag{19}$$

quadratic. Making use of (8) and its first three derivatives with respect to x, $\boldsymbol{F}_{xa}^*$ is obtained as follows:

$$\boldsymbol{F}_{xa}^* = \left[\begin{array}{cccc|c} \mu_1(x,\lambda) & \mu_2(x,\lambda) & \mu_3(x,\lambda) & \mu_4(x,\lambda) & d(\lambda)\mu_5(x,\lambda) \\ \mu_1'(x,\lambda) & \mu_2'(x,\lambda) & \mu_3'(x,\lambda) & \mu_4'(x,\lambda) & d(\lambda)\mu_5'(x,\lambda) \\ \mu_1''(x,\lambda) & \mu_2''(x,\lambda) & \mu_3''(x,\lambda) & \mu_4''(x,\lambda) & d(\lambda)\mu_5''(x,\lambda) \\ \mu_1'''(x,\lambda) & \mu_2'''(x,\lambda) & \mu_3'''(x,\lambda) & \mu_4'''(x,\lambda) & d(\lambda)\mu_5'''(x,\lambda) \\ \hline 0 & 0 & 0 & 0 & 1 \end{array}\right] \tag{20}$$

The constitutive equations are cast in matrix form analogous to (19):

$$\boldsymbol{\vartheta}_x = \boldsymbol{P}_x \cdot \boldsymbol{Z}_x \tag{21}$$

with

$$\boldsymbol{Z}_x^T = \lfloor \vartheta(x,\lambda), M_{Tp}(x,\lambda), M_\omega(x,\lambda), M_{Ts}(x,\lambda) | 1 \rfloor, \tag{22}$$

where M_{Tp}, M_ω, and M_{Ts} denote the primary torque, the warping moment, and the secondary torque, respectively, and

$$\boldsymbol{P}_x = \left[\begin{array}{cccc|c} 1 & 0 & 0 & 0 & 0 \\ 0 & \dfrac{1}{GI_T} & 0 & 0 & 0 \\ 0 & 0 & -\dfrac{1}{GI_\omega} & 0 & 0 \\ 0 & 0 & 0 & -\dfrac{1}{GI_\omega} & 0 \\ \hline 0 & 0 & 0 & 0 & 1 \end{array}\right], \tag{23}$$

containing the compliances $1/GI_T$ and $1/GI_\omega$. The purpose of the last coefficient in (22) is to render the matrix $\boldsymbol{P}_x$ quadratic. Solving (21) for $\boldsymbol{Z}_x$, considering (19) and a relation for $\boldsymbol{\vartheta}_x$ analogous to (21), results in

$$\boldsymbol{Z}_x = \boldsymbol{P}_x^{-1} \cdot \boldsymbol{\vartheta}_x = \boldsymbol{P}_x^{-1} \cdot \boldsymbol{F}_{xa}^* \cdot \boldsymbol{\vartheta}_a = \boldsymbol{P}_x^{-1} \cdot \boldsymbol{F}_{xa}^* \cdot \boldsymbol{P}_x \cdot \boldsymbol{Z}_a = \boldsymbol{F}_{xa} \cdot \boldsymbol{Z}_a\,, \tag{24}$$

where

$$\boldsymbol{F}_{xa} = \boldsymbol{P}_x^{-1} \cdot \boldsymbol{F}_{xa}^* \cdot \boldsymbol{P}_x \tag{25}$$

is referred to as transfer matrix.

4. Secant Stiffness Matrix

Specialization of (19) for $x = l$ yields

$$\boldsymbol{\vartheta}_b = \boldsymbol{F}_{ba}^* \cdot \boldsymbol{\vartheta}_a. \tag{26}$$

Exchanging the first two rows in (26) and replacing ϑ_a'' by $-\vartheta_a''$, ϑ_a''' by $-\vartheta_a'''$, ϑ_b' by $-\vartheta_b'$, and ϑ_b'' by $-\vartheta_b'''$ in order to comply with the sign convention of the displacement method, gives

$$\bar{\boldsymbol{\vartheta}}_a^T = \lfloor \vartheta_a'(\lambda),\, \vartheta_a(\lambda), -\vartheta_a''(\lambda), -\vartheta_a'''(\lambda) \mid 1 \rfloor \tag{27}$$

$$\bar{\boldsymbol{\vartheta}}_b^T = \lfloor -\vartheta_b'(\lambda),\, \vartheta_b(\lambda), \vartheta_b''(\lambda), -\vartheta_b'''(\lambda) \mid 1 \rfloor. \tag{28}$$

Accordingly, the matrix $\bar{\boldsymbol{F}}_{ba}^*$ in the relation

$$\bar{\boldsymbol{\vartheta}}_b = \bar{\boldsymbol{F}}_{ba}^* \cdot \bar{\boldsymbol{\vartheta}}_a \tag{29}$$

is obtained as

$$\bar{\boldsymbol{F}}_{ba}^* = \left[\begin{array}{cccc|c} -\mu_2'(\lambda) & -\mu_1'(\lambda) & \mu_3'(\lambda) & \mu_4'(\lambda) & -d(\lambda)\mu_5'(\lambda) \\ \mu_2(\lambda) & \mu_1(\lambda) & -\mu_3(\lambda) & -\mu_4'(\lambda) & d(\lambda)\mu_5(\lambda) \\ -\mu_1''(\lambda) & -\mu_2''(\lambda) & \mu_3''(\lambda) & \mu_4''(\lambda) & -d(\lambda)\mu_5''(\lambda) \\ \mu_1'''(\lambda) & \mu_2'''(\lambda) & -\mu_3'''(\lambda) & -\mu_4'''(\lambda) & d(\lambda)\mu_5'''(\lambda) \\ \hline 0 & 0 & 0 & 0 & 1 \end{array}\right] \tag{30}$$

In the terms in (30) with the letter symbol μ the argument $x=l$ was omitted.

The first two lines of (29) can be written as

$$\boldsymbol{q}_b = \boldsymbol{T}_{ba}^{(1)} \cdot \boldsymbol{q}_a + \boldsymbol{T}_{ba}^{(2)} \cdot \boldsymbol{s}_a + \boldsymbol{t}_{ba}, \tag{31}$$

where

$$\boldsymbol{q}_a = \begin{Bmatrix} \vartheta_a'(\lambda) \\ \vartheta_a(\lambda) \end{Bmatrix}, \quad \boldsymbol{q}_b = \begin{Bmatrix} -\vartheta_b'(\lambda) \\ \vartheta_b(\lambda) \end{Bmatrix}, \tag{32}$$

$$\boldsymbol{s}_a = \begin{Bmatrix} -\vartheta_a''(\lambda) \\ -\vartheta_a'''(\lambda) \end{Bmatrix}, \tag{33}$$

$$\boldsymbol{T}_{ba}^{(1)} = \begin{bmatrix} -\mu_2'(\lambda) & -\mu_1'(\lambda) \\ \mu_2(\lambda) & \mu_1(\lambda) \end{bmatrix},$$

$$\boldsymbol{T}_{ba}^{(2)} = \begin{bmatrix} \mu_3'(\lambda) & \mu_4'(\lambda) \\ -\mu_3(\lambda) & -\mu_4(\lambda) \end{bmatrix} \tag{34}$$

and

$$\boldsymbol{t}_{ba} = \begin{Bmatrix} -d(\lambda)\,\mu_5'(\lambda) \\ d(\lambda)\mu_5(\lambda) \end{Bmatrix}. \tag{35}$$

Solving (31) for $\boldsymbol{s}_a$ gives

$$\boldsymbol{s}_a = \boldsymbol{K}_{as} \cdot \boldsymbol{q}_a + \boldsymbol{K}_{ab} \cdot \boldsymbol{q}_b + \boldsymbol{s}_{ab}, \tag{36}$$

where

$$\boldsymbol{K}_{as} = -\left(\boldsymbol{T}_{ba}^{(2)}\right)^{-1} \cdot \boldsymbol{T}_{ba}^{(1)},$$

$$\boldsymbol{K}_{ab} = \left(\boldsymbol{T}_{ba}^{(2)}\right)^{-1}, \tag{37}$$

and

$$\boldsymbol{s}_{ab} = -\left(\boldsymbol{T}_{ba}^{(2)}\right)^{-1} \cdot \boldsymbol{t}_{ba}\,. \tag{38}$$

Inversion of (29) yields

$$\bar{\boldsymbol{\vartheta}}_a = (\bar{\boldsymbol{F}}_{ba}^*)^{-1} \cdot \bar{\boldsymbol{\vartheta}}_b, \tag{39}$$

where

$$(\bar{\boldsymbol{F}}_{ba}^*)^{-1} = \left[\begin{array}{cccc|c} t_{11}(\lambda) & t_{12}(\lambda) & t_{13}(\lambda) & t_{14}(\lambda) & t_{15}(\lambda) \\ t_{21}(\lambda) & t_{22}(\lambda) & t_{23}(\lambda) & t_{24}(\lambda) & t_{25}(\lambda) \\ t_{31}(\lambda) & t_{32}(\lambda) & t_{33}(\lambda) & t_{34}(\lambda) & t_{35}(\lambda) \\ t_{41}(\lambda) & t_{42}(\lambda) & t_{43}(\lambda) & t_{44}(\lambda) & t_{45}(\lambda) \\ \hline 0 & 0 & 0 & 0 & 1 \end{array}\right]. \tag{40}$$

Analogous to (31), the first two rows of (39) can be written as

$$\boldsymbol{q}_a = \boldsymbol{T}_{ab}^{(1)} \cdot \boldsymbol{q}_b + \boldsymbol{T}_{ab}^{(2)} \cdot \boldsymbol{s}_b + \boldsymbol{t}_{ab} \tag{41}$$

where

$$\boldsymbol{s}_b = \begin{Bmatrix} \vartheta_b''(\lambda) \\ -\vartheta_b'''(\lambda) \end{Bmatrix}, \tag{42}$$

$$\boldsymbol{T}_{ab}^{(1)} = \begin{bmatrix} t_{11}(\lambda) & t_{12}(\lambda) \\ t_{21}(\lambda) & t_{22}(\lambda) \end{bmatrix},$$

$$\boldsymbol{T}_{ab}^{(2)} = \begin{bmatrix} t_{13}(\lambda) & t_{14}(\lambda) \\ t_{23}(\lambda) & t_{24}(\lambda) \end{bmatrix}, \tag{43}$$

$$\boldsymbol{t}_{ab} = \begin{Bmatrix} t_{15}(\lambda) \\ t_{25}(\lambda) \end{Bmatrix}. \tag{44}$$

Solving (42) for $\boldsymbol{s}_b$ gives

$$\boldsymbol{s}_b = \boldsymbol{K}_{bs} \cdot \boldsymbol{q}_b + \boldsymbol{K}_{ba} \cdot \boldsymbol{q}_a + \boldsymbol{s}_{ba}\,, \tag{45}$$

where

$$\boldsymbol{K}_{bs} = -\left(\boldsymbol{T}_{ab}^{(2)}\right)^{-1} \cdot \boldsymbol{T}_{ab}^{(1)}, \boldsymbol{K}_{ba} = \left(\boldsymbol{T}_{ab}^{(2)}\right)^{-1}, \tag{46}$$

and

$$\boldsymbol{s}_{ba} = -\left(\boldsymbol{T}_{ab}^{(2)}\right)^{-1} \cdot \boldsymbol{t}_{ab}\,. \tag{47}$$

Combining (36) and (45) results in

$$\boldsymbol{K}_S \cdot \boldsymbol{q} = \boldsymbol{P}, \tag{48}$$

where, in the terminology of the FEM,

$$\boldsymbol{K}_S = \left[\begin{array}{c|c} \boldsymbol{K}_{as} & \boldsymbol{K}_{ab} \\ \hline \boldsymbol{K}_{ba} & \boldsymbol{K}_{bs} \end{array}\right] \tag{49}$$

represents the secant stiffness matrix for the given system, considered as a single finite element,

$$\boldsymbol{q} = \begin{Bmatrix} \boldsymbol{q}_a \\ \hline \boldsymbol{q}_b \end{Bmatrix} \tag{50}$$

is the vector of nodal “displacements”, and

$$\boldsymbol{P} = \begin{Bmatrix} \boldsymbol{s}_a - \boldsymbol{s}_{ab} \\ \hline \boldsymbol{s}_b - \boldsymbol{s}_{ba} \end{Bmatrix} \tag{51}$$

stands for a vector of nodal “forces”. Hence (48) represents the equilibrium equation.

Lateral torsional buckling occurs for the smallest value of λ, λ_S, for which

$$Det\ \boldsymbol{K}_S = 0. \tag{52}$$

The eigenvector $\boldsymbol{v}_1$, corresponding to the eigenvalue $\lambda_S = \lambda_1$, follows from

$$\boldsymbol{K}_S(\lambda_1) \cdot \boldsymbol{v}_1 = \boldsymbol{0}. \tag{53}$$

For $\lambda \to \lambda_S$, $\boldsymbol{q}(x, \lambda) \to \infty$, $0 < x < l$, which is in contradiction to the assumption of small prebuckling rotations (see (4)). An analogous contradiction occurs if a simply supported beam, subjected to eccentric compressive forces at both ends, is analyzed by means of second-order theory. As these forces approach the Euler load, the displacements tend to infinity.

5. Consistently Linearized Eigenproblem

The mathematical formulation of the consistently linearized eigenproblem reads [3]

$$[\boldsymbol{K}_T + (\lambda^* - \lambda)\, \boldsymbol{K}_{T,\lambda}] \cdot \boldsymbol{v}^* = \boldsymbol{0}\,, \tag{54}$$

where $\boldsymbol{K}_T$ is the $[N \times N]$ tangent stiffness matrix in the frame of the FEM and $\boldsymbol{K}_{T,\lambda}$ is its first derivative with respect to λ along a direction parallel to the primary path. $\boldsymbol{v}_1^*, \boldsymbol{v}_2^*, \ldots, \boldsymbol{v}_N^*$ are the eigenvectors corresponding to the distinct eigenvalues $\lambda_1^* - \lambda$, $\lambda_2^* - \lambda$,..., $\lambda_N^* - \lambda$. Writing (3) for the first eigenpair $(\lambda_1^* - \lambda,\ \boldsymbol{v}_1^*)$, gives

$$[\boldsymbol{K}_T + (\lambda_1^* - \lambda)\, \boldsymbol{K}_{T,\lambda}] \cdot \boldsymbol{v}_1^* = \boldsymbol{0}. \tag{55}$$

Specialization of (55) for the stability limit $(\lambda_1^* - \lambda = 0,\ \boldsymbol{v}_1^* = \boldsymbol{v}_1)$, where $\lambda = \lambda_S$, yields

$$\boldsymbol{K}_T \cdot \boldsymbol{v}_1 = \boldsymbol{0}. \tag{56}$$

Originally, the consistently linearized eigenproblem was used as a tool for circumventing numerical problems in the vicinity of snap – through points and bifurcation points on nonlinear primary paths. More recently, this eigenproblem was employed for derivation of subsidiary conditions for buckling at special prebuckling states, such as, e.g. , membrane stress states.

In the following, it will be shown that for lateral torsional buckling the eigensolution obtained from

$$[\boldsymbol{K}_S + (\tilde{\lambda}_1 - \lambda)\, \boldsymbol{K}_{S,\lambda}] \cdot \tilde{\boldsymbol{v}}_1 = \boldsymbol{0} \tag{57}$$

is the same as the one resulting from (55), i.e.,

$$\lambda_1^*(\lambda) = \tilde{\lambda}_1(\lambda), \quad \boldsymbol{v}_1^*(\lambda) = \tilde{\boldsymbol{v}}_1(\lambda). \tag{58}$$

The reason for this remarkable result is that for lateral torsional buckling,

$$\boldsymbol{v}_1^*(\lambda) = \tilde{\boldsymbol{v}}_1(\lambda) = \boldsymbol{v}_1 = \mathbf{const}\,. \tag{59}$$

which, e.g., is not the case for torsional flexural buckling. Consideration of (59) in (55) and (57), premultiplication of the resulting relations by $\boldsymbol{v}_1$, and combination of the so-obtained equations, considering (58.1), gives

$$\frac{\boldsymbol{v}_1 \cdot \boldsymbol{K}_S \cdot \boldsymbol{v}_1}{\boldsymbol{v}_1 \cdot \boldsymbol{K}_{S,\lambda} \cdot \boldsymbol{v}_1} = \frac{\boldsymbol{v}_1 \cdot \boldsymbol{K}_T \cdot \boldsymbol{v}_1}{\boldsymbol{v}_1 \cdot \boldsymbol{K}_{T,\lambda} \cdot \boldsymbol{v}_1}. \tag{60}$$

As follows from (53) and (56), (60) is satisfied at the stability limit. To check whether this relation is also fulfilled for λ=0, (48) is derived with respect to λ:

$$\boldsymbol{K}_{S,\lambda} \cdot \boldsymbol{q} + \boldsymbol{K}_S \cdot \boldsymbol{q}_{,\lambda} = \boldsymbol{P}_{,\lambda}\,, \tag{61}$$

where

$$\boldsymbol{P}_{,\lambda} = \boldsymbol{K}_T \cdot \boldsymbol{q}_{,\lambda} \tag{62}$$

represents the rate form of the equilibrium equations. Specialization of (61) for $\lambda = 0 \rightarrow \boldsymbol{q} = \boldsymbol{0}$ obviously yields

$$\boldsymbol{K}_S = \boldsymbol{K}_T\,. \tag{63}$$

Combination of (61) and (62), followed by derivation with respect to λ, results in

$$\boldsymbol{K}_{S,\lambda\lambda} \cdot \boldsymbol{q} + 2\boldsymbol{K}_{S,\lambda} \cdot \boldsymbol{q}_{,\lambda} + \boldsymbol{K}_S \cdot \boldsymbol{q}_{,\lambda\lambda} =$$

$$\boldsymbol{K}_{T,\lambda} \cdot \boldsymbol{q}_{,\lambda} + \boldsymbol{K}_T \cdot \boldsymbol{q}_{,\lambda\lambda}\,. \tag{64}$$

Specialization of (64) for λ=0 including consideration of (63) gives

$$2\boldsymbol{K}_{S,\lambda} = \boldsymbol{K}_{T,\lambda}. \tag{65}$$

As follows from (63) and (65) and from the positive definiteness $\boldsymbol{K}_T(\lambda{=}0){=}\boldsymbol{K}_0$, where $\boldsymbol{K}_0$ is the constant small – displacement stiffness matrix [7], satisfaction of (60) requires

$$\boldsymbol{K}_{S,\lambda} \cdot \boldsymbol{v}_1 = \boldsymbol{0} \quad \Leftrightarrow \quad \boldsymbol{K}_{T,\lambda} \cdot \boldsymbol{v}_1 = \boldsymbol{0}\,. \tag{66}$$

Specialization of (55) and (57) for $\lambda = 0$ and consideration of (59) and (66) yields

$$\tilde{\lambda}_1(\lambda = 0) = \lambda_1^*(\lambda = 0) = \infty. \tag{67}$$

In Chapter 6, (67) will be verified numerically.

For lateral torsional buckling, the eigenproblem (57) which is based on an analytical result for the secant stiffness matrix $\boldsymbol{K}_S$ is superior to the eigenproblem (55) in the frame of the FEM. Hence, there is no need to use (55) for numerical verification of subsidiary conditions for lateral torsional buckling, hypothesized by means of this relation.

The basis for derivation of such conditions is the relation

$$\left([\boldsymbol{K}_T + (\lambda_1^* {-} \lambda)\, \boldsymbol{K}_{T,\lambda}] \cdot \boldsymbol{v}_1^*\right)_{,\lambda\lambda\lambda}\Big|_{\lambda=\lambda_S} = \boldsymbol{0}\,, \tag{68}$$

resulting in [1]

$$\lambda^*_{1,\lambda\lambda\lambda} = -3\lambda^{*2}_{1,\lambda\lambda} + 2\frac{\boldsymbol{v}_1 \cdot \boldsymbol{K}_{T,\lambda\lambda\lambda} \cdot \boldsymbol{v}_1}{\boldsymbol{v}_1 \cdot \boldsymbol{K}_{T,\lambda} \cdot \boldsymbol{v}_1}. \tag{69}$$

For buckling at general stress states, characterized by a percentage bending energy of the strain energy that increases in the prebuckling regime with increasing λ,

$$\lambda^*_{1,\lambda\lambda\lambda} > 0. \tag{70}$$

For buckling at special stress states, characterized by a constant percentage strain energy in the prebuckling regime,

$$\lambda^*_{1,\lambda\lambda\lambda} = 0, \tag{71}$$

with the exception of buckling from a membrane stress state, for which

$$\lambda^*_{1,\lambda\lambda\lambda} \leq 0\,. \tag{72}$$

Hence, according to the above hypotheses, for lateral torsional buckling, characterized by 100% of percentage bending energy of the strain energy in the prebuckling regime,

$$\lambda^{*2}_{1,\lambda\lambda} = \frac{2}{3}\frac{\boldsymbol{v}_1 \cdot \boldsymbol{K}_{T,\lambda\lambda\lambda} \cdot \boldsymbol{v}_1}{\boldsymbol{v}_1 \cdot \boldsymbol{K}_{T,\lambda} \cdot \boldsymbol{v}_1}, \tag{73}$$

as follows from substitution of (71) into (69).

Lateral torsional buckling represents a limiting case of torsional flexural buckling for which (70) holds. By contrast, lateral buckling is no limiting case of buckling at a constant percentage bending energy of the total strain energy in the prebuckling regime. This fact is reflected by different signs of the curvatures of the eigenvalue curves $\lambda_1^*(\lambda)$ at the stability limit where $\lambda_{1,\lambda}^* = 0$ [1]. (For convenience, $\lambda_1^*(\lambda)$ is occasionally referred to as the eigenvalue curve, although $\lambda_1^* - \lambda$ is actually the eigenvalue.) Lateral torsional buckling is the only case of (71) for which

$$\lambda_{1,\lambda\lambda}^* > 0 \tag{74}$$

holds in (73). In Chapter 6, (74) will be verified numerically.

6. Numerical Investigation

6.1 Solution of the eigenproblem

The numerical investigation consists of stability analysis of a beam as shown in Fig. 1. The structural steel shape is a HE-A 200 [8]. The input data for the analysis are given as follows:

$l = 2\text{m}$,

$I_y = 3690 \cdot 10^{-8}\text{m}^4$, $I_z = 1340 \cdot 10^{-8}\text{m}^4$,

$I_T = 21.1 \cdot 10^{-8}\text{m}^4$, $I_\omega = 10.8 \cdot 10^{-8}\text{m}^6$,

$E = 21 \cdot 10^7\text{kN/m}^2$, $\nu = 0.3$,

$\bar{M}_y = 80$ kNm, $\bar{M}_z = 1$ kNm.

Because of $\bar{M}_z \neq 0$, the deformed axis of the beam is a space curve. Since, $\bar{M}_z/\bar{M}_y = 1/80$, the deviation of this curve from the plane curve that would be obtained for $\bar{M}_z = 0$ is small, representing an imperfection that is characterized by a prebuckling rotation ϑ of the cross-section of the beam about the x-axis (Fig. 2).

The boundary conditions of the fork-supported beam are given as

$$\vartheta_a = \vartheta_b = 0, \tag{75}$$

and

$$M_{\omega,a} = -EI_\omega \vartheta_a'' = 0 \quad \Rightarrow \quad \vartheta_a'' = 0,$$
$$M_{\omega,b} = -EI_\omega \vartheta_b'' = 0 \quad \Rightarrow \quad \vartheta_b'' = 0. \tag{76}$$

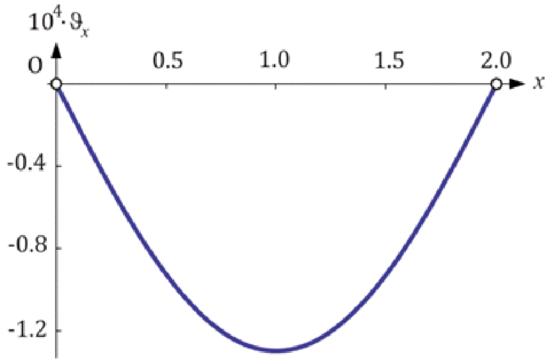

Fig. 3. $\vartheta(x,\lambda=1)$.

To compute $\boldsymbol{\vartheta}_x$, $\boldsymbol{Z}_x$ must be known (see (21)). Determination of $\boldsymbol{Z}_x$ requires knowledge of $\boldsymbol{Z}_a$ (see (24)). The transpose of $\boldsymbol{Z}_a$ follows from specialization of (22) for $x = 0$. Considering the boundary conditions at this point, $\boldsymbol{Z}_a^T$ is obtained as

$$\boldsymbol{Z}_a^T = \lfloor 0,\ M_{Tp,a},\ 0,\ M_{Ts,a} \mid 1 \rfloor. \tag{77}$$

Use of the first and the third line of the transfer matrix $\boldsymbol{F}_{ba}$ gives

$$\begin{bmatrix} F_{ba,12}(\lambda) & F_{ba,14}(\lambda) \\ F_{ba,32}(\lambda) & F_{ba,34}(\lambda) \end{bmatrix} \begin{Bmatrix} M_{Tp,a}(\lambda) \\ M_{Ts,a}(\lambda) \end{Bmatrix} = \begin{Bmatrix} -F_{ba,15}(\lambda) \\ -F_{ba,35}(\lambda) \end{Bmatrix} \tag{78}$$

which can be solved for $M_{Tp,a}$ and $M_{Ts,a}$.

Fig. 3 shows the function $\vartheta(x,\lambda)$, evaluated for $\lambda = 1$, i.e., for the reference moments $\bar{M}_y$ and $\bar{M}_z$ (see (1) and (2)).

Since $\vartheta(x,\lambda)$ is symmetric with respect to midspan, so are M_η and M_ζ (see (5)) and

$$M_\omega = -EI_\omega \vartheta''. \tag{79}$$

Table 1 contains the results for M_η and M_ζ at five points in the interval <0, 2.0>. The deviations of M_η from $\bar{M}_y = 80$ kNm and of M_ζ from $\bar{M}_z = 1$ kNm are small.

Symmetry of M_η and M_ζ entails symmetry of w and v.

Since

$$M_{Tp} = GI_T\vartheta',\ M_{Ts} = -EI_\omega \vartheta''' \tag{80}$$

are antisymmetric with respect to midspan, so is

$$M_T = M_{Tp} + M_{Ts}. \tag{81}$$

Table 1. $M_\eta(x, \lambda=1)$, $M_\zeta(x, \lambda=1)$

x [m]	M_η [kNm]	M_ζ [kNm]
0.0	80	1
0.5	79.99991	1.00737
1.0	79.99987	1.01032
1.5	79.99991	1.00737
2.0	80	1

Since $\vartheta_a'(\lambda)$ tends to infinity as λ approaches λ_S (see Fig.4), so does $M_{Tp,a}(\lambda)$. By analogy, in this case also $M_{Ts,a}(\lambda)$ tends to infinity. This characteristic feature of second-order theory has no influence on the following solution of the underlying eigenproblem.

The zeros of the determinant of the coefficient matrix

$$\boldsymbol{U}(\lambda)=\begin{bmatrix} F_{ba,12}(\lambda) & F_{ba,14}(\lambda) \\ F_{ba,32}(\lambda) & F_{ba,34}(\lambda) \end{bmatrix} \tag{82}$$

in (78) are the eigenvalues of the underlying eigenproblem. The first two eigenvalues are obtained as λ_1=8.899 and λ_2=32.331. λ_1=λ_S is the load factor that defines the buckling moment $\lambda_S \bar{M}_z$. Fig. 5 shows the corresponding eigenform, representing a spatial halfwave. To obtain this eigenform requires specification of the symmetry condition

$$\hat{\vartheta}_a' = -\hat{\vartheta}_b' \,. \tag{83}$$

Herein, $\hat{\vartheta}_a'$ is chosen as 1.

Fig. 6 shows the eigenform corresponding to λ_2, consisting of two spatial halfwaves. To obtain this eigenform requires specification of the antisymmetry condition

$$\hat{\vartheta}_a' = \hat{\vartheta}_b' \,. \tag{84}$$

To verify that the zeros of the determinant of the

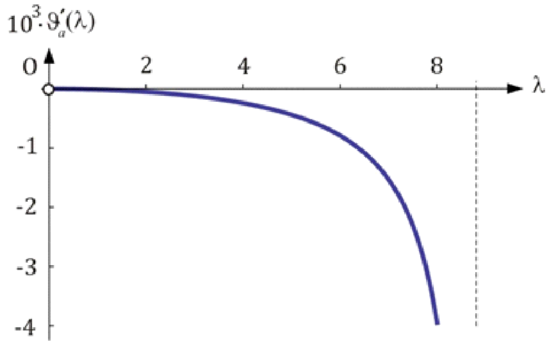

Fig. 4. $\vartheta_a'(\lambda)$

secant stiffness matrix $\boldsymbol{K}_S$ (see (49)) are identical with the zeros of the determinant of the matrix U (see (82)), the boundary conditions

$$\hat{\vartheta}_a = \hat{\vartheta}_b = 0 \tag{85}$$

for the eigenform must be considered. Accordingly, the number of the elements of the eigenvector is reduced from four to two, resulting in

$$\hat{\boldsymbol{v}}=\begin{Bmatrix} \hat{\vartheta}_a' \\ -\hat{\vartheta}_b' \end{Bmatrix}. \tag{86}$$

The minus sign in (86) correlates with the minus sign in the expression for $\boldsymbol{q}_b$ (see (32)). Because of the reduction of the eigenvector, the secant stiffness matrix $\boldsymbol{K}_S$ must be reduced from a [4 × 4] to a [2 × 2] submatrix:

$$\hat{\boldsymbol{K}}_S(\lambda)=\begin{bmatrix} K_{11}(\lambda) & K_{13}(\lambda) \\ K_{31}(\lambda) & K_{33}(\lambda) \end{bmatrix}. \tag{87}$$

Although $Det\,\hat{\boldsymbol{K}}_S(\lambda)$ is different from $Det\,\boldsymbol{U}(\lambda)$ (see Fig.7), the first two zeros of $Det\,\hat{\boldsymbol{K}}_S(\lambda)$ were found to agree with the corresponding zeros of $Det\,\boldsymbol{U}(\lambda)$.

The location of the vertical asymptote of the function $Det\,\hat{\boldsymbol{K}}_S(\lambda)$ between its first and second zero

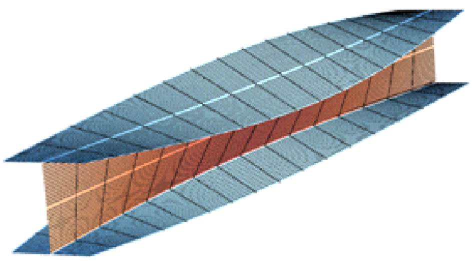

Fig. 5. First eigenform (buckling mode)

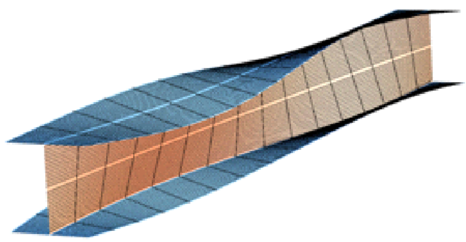

Fig. 6. Second eigenform

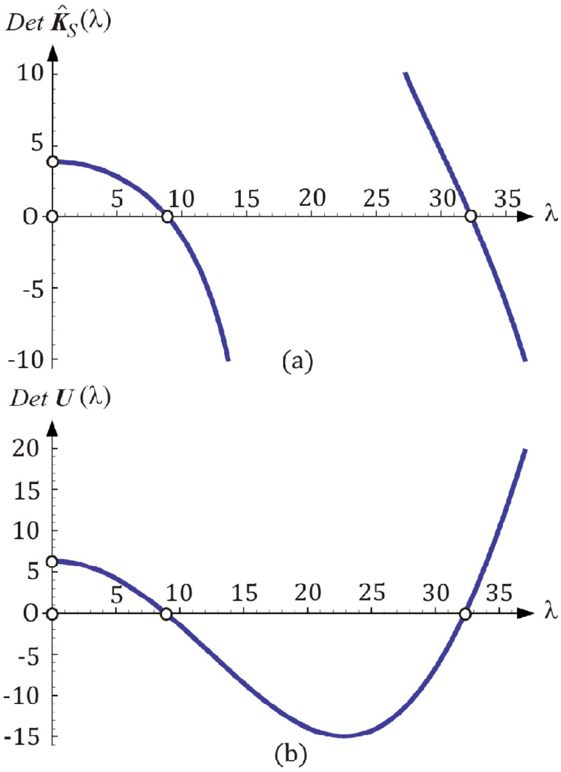

Fig. 7. (a) $Det\,\hat{K}_S(\lambda)$, (b) $Det\,U(\lambda)$

agrees with the location of the point of intersection of the mechanically insignificant second branch of the load-displacement curves, consisting of infinitely many branches, with the λ-axis. This follows from inversion of (48), resulting in

$$q = \hat{K}_S^{-1} \cdot P, \quad Det\,\hat{K}_S \neq 0, \tag{88}$$

where

$$\hat{K}_S^{-1} = \frac{\left(Adj\,\hat{K}_S\right)^T}{Det\,\hat{K}_S}. \tag{89}$$

For

$$Det\,\hat{K}_S = \infty, \tag{90}$$

$$\hat{K}_S^{-1} = \mathbf{0} \quad \Rightarrow \quad q = \mathbf{0}. \tag{91}$$

6.2. Characteristics of the consistently linearized eigenproblem

Formulation of the consistently linearized eigenproblem on the basis of $\hat{K}_S(\lambda)$ and $\hat{v}$ gives

$$[\hat{K}_S + (\tilde{\lambda} - \lambda)\hat{K}_{S,\lambda}] \cdot \hat{v} = 0, \tag{92}$$

where

$$\hat{v} = \begin{Bmatrix} \hat{\vartheta}'_a \\ -\hat{\vartheta}'_b \end{Bmatrix}. \tag{93}$$

Normalization of $\hat{v}$ such that

$$\hat{v} \cdot \hat{v} = 1 \tag{94}$$

yields

$$|\hat{v}| = \sqrt{\left(\hat{\vartheta}'_a\right)^2 + \left(-\hat{\vartheta}'_b\right)^2} = 1. \tag{95}$$

The solution of (92) consists of two eigenpairs:

$$\left(\tilde{\lambda}_1 - \lambda,\ \hat{v}_1\right), \quad \left(\tilde{\lambda}_2 - \lambda,\ \hat{v}_2\right). \tag{96}$$

The first eigenpair refers to symmetric eigenforms, for which

$$\hat{\vartheta}'_a = -\hat{\vartheta}'_b, \tag{97}$$

resulting in

$$\hat{v}_1 = \frac{1}{\sqrt{2}} \begin{Bmatrix} 1 \\ 1 \end{Bmatrix} = \mathbf{const}. \tag{98}$$

The second eigenpair refers to antisymmetric eigenforms, for which

$$\hat{\vartheta}'_a = \hat{\vartheta}'_b, \tag{99}$$

resulting in

$$\hat{v}_2 = \frac{1}{\sqrt{2}} \begin{Bmatrix} 1 \\ -1 \end{Bmatrix} = \mathbf{const}. \tag{100}$$

The independence of $\hat{v}_1$ and $\hat{v}_2$ of λ verifies (59). The two eigenvectors satisfy the orthogonality condition

$$\hat{v}_1 \cdot \hat{v}_2 = 0. \tag{101}$$

$\hat{K}_S(\lambda)$ is an ingredient of an analytical solution of the underlying eigenproblem. Hence,

$$Det\,\hat{K}_S(\lambda) = 0 \tag{102}$$

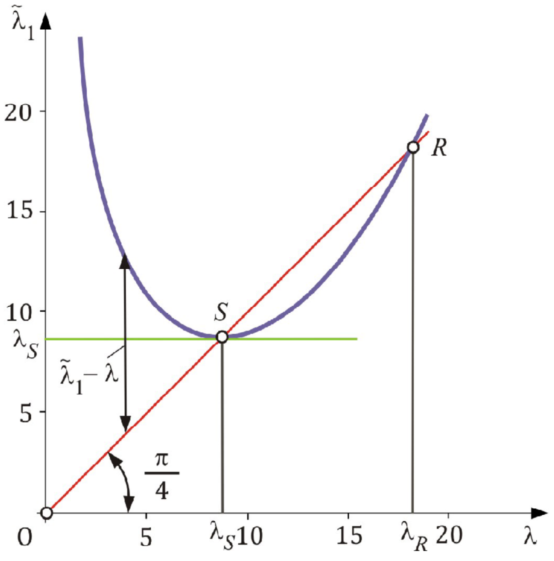

Fig. 8. $\tilde{\lambda}_1(\lambda)$

for countably infinitely many values of $\lambda > 0$, associated with zero eigenvalues

$$\tilde{\lambda}_1 - \lambda = 0, \tag{103}$$

and

$$\tilde{\lambda}_2 - \lambda = 0. \tag{104}$$

The smallest zero eigenvalue represents the stability limit $\lambda = \lambda_S = \tilde{\lambda}_1$ and, thus, defines the buckling moment $\lambda_S \bar{M}_y$. Fig. 8 illustrates the function $\tilde{\lambda}_1(\lambda)$.

Fig. 8 confirms $\tilde{\lambda}_{1,\lambda}(\lambda_S) = 0$ [1] and verifies the hypotheses $\tilde{\lambda}_{1,\lambda\lambda}(\lambda_S) > 0$ (see (74), recalling that $\lambda_1^* = \tilde{\lambda}_1$) and $\tilde{\lambda}_1(0) = \infty$ (see (67)). Closer inspection of $\tilde{\lambda}_1(\lambda)$ also seems to confirm the hypothesis that the curvature of this curve becomes a minimum at *S*, which implies $\tilde{\lambda}_{1,\lambda\lambda\lambda}(\lambda_S)$=0 (see (71)).

Continuation of the curve $\tilde{\lambda}_1(\lambda)$ beyond $\lambda = \lambda_S$ shows that (103) also holds at $\lambda = \lambda_R$, although

$$\tilde{\lambda}_{1,\lambda}(\lambda_R) \neq 0. \tag{105}$$

For $\lambda \to \lambda_R$,

$$Det\, \hat{\boldsymbol{K}}_S(\lambda) \to -\infty \tag{106}$$

(see Fig 9(a)). Specialization of (92) for $\lambda = \lambda_R$ and premultiplication of the obtained relation by $\hat{\boldsymbol{v}}_1$ gives

$$\lambda_R - \lambda = -\frac{\hat{\boldsymbol{v}}_1 \cdot \hat{\boldsymbol{K}}_S(\lambda_R) \cdot \hat{\boldsymbol{v}}_1}{\hat{\boldsymbol{v}}_1 \cdot \hat{\boldsymbol{K}}_{S,\lambda}(\lambda_R) \cdot \hat{\boldsymbol{v}}_1} = -\frac{(-\infty)}{(-\infty)} = -0, \tag{107}$$

because the quadratic form in the denominator in (107) is tending more strongly to $-\infty$ than the one in the numerator (Fig. 9). The mathematical meaning of λ_R ($\boldsymbol{q}(\lambda_R)$=0) was explained in the last paragraph of Subchapter 6.1.

7. Conclusions

• Remarkably, the solution of the consistently linearized eigenproblem for lateral torsional buckling, formulated by means of an analytical representation of the secant stiffness matrix, is identical with the

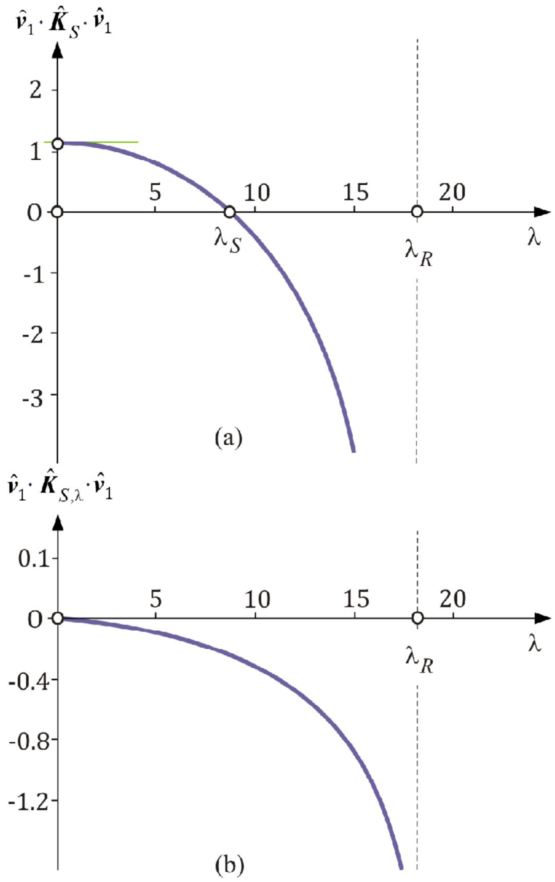

Fig. 9. (a) $\hat{\boldsymbol{v}}_1 \cdot \hat{\boldsymbol{K}}_S(\lambda) \cdot \hat{\boldsymbol{v}}_1$, (b) $\hat{\boldsymbol{v}}_1 \cdot \hat{\boldsymbol{K}}_{S,\lambda}(\lambda) \cdot \hat{\boldsymbol{v}}_1$.

one resulting from formulation of such an eigenproblem with the help of the tangent stiffness matrix. The latter represents an essential ingredient of nonlinear FEA. The secant stiffness matrix was derived by means of the transfer matrix method.

• Characteristics of the eigenvalue curve $\lambda_1^*(\lambda)$ resulting from the consistently linearized eigenproblem are

(a) a minimum of the curvature of this curve at the stability limit where $\lambda_1^* = \lambda_S$, and $\lambda_{1,\lambda}^*(\lambda_S) = 0$, $\lambda_{1,\lambda\lambda}^*(\lambda_S) > 0$, and

(b) a vertical asymptote of the curve at λ=0, i.e.,

$$\lambda_1^*(\lambda = 0) = \infty.$$

The characteristic feature of the eigenvector function $\boldsymbol{v}_1^*(\lambda)$ is its constancy. Hence, the solution of the consistently linearized eigenproblem applied to lateral torsional buckling takes up a position between the general case, where both the eigenvalue and the eigenvector function are variables, and the special case of linear stability problems, where both are constants.

• The presented solution closes a gap in a new concept of categorization of buckling by means of spherical geometry.

მექანიკა

საკუთრივი მნიშვნელობის ამოცანის თანმიმდევრობითი გაწრფივების დახასიათება ღუნვის გვერდითი გრეხვისათვის

მ. ამინბაგაი* და ჰ. ა. მანგი*

** ვენის ტექნოლოგიური უნივერსიტეტის მასალათა და სტრუქტურების მექანიკის ინსტიტუტი, ვენა, ავსტრია*

საკუთრივი მნიშვნელობის ამოცანის თანმიმდევრობით გაწრფივება მძლავრი მათემატიკური იარაღი აღმოჩნდა ღუნვების კლასიფიკაციისათვის. განსაკუთრებით საინტერესოა პრეღუნვის მდგომარეობები მუდმივი სრული ენერგიით. ასეთი მდგომარეობის ორი ზღვრული შემთხვევაა მებრანის დაძაბულობისა და წმინდა ღუნვების მდგომარეობები. კვლევის საგანია წმინდა ღუნვების მდგრადობა, რომელიც გვერდითი ღუნვის გრეხვად იწოდება. ტრანსფერ-მატრიცის მეთოდი გამოიყენება ანალიზური სახით სიმტკიცის მატრიცის მისაღებად. საკუთრივი ფუნქციის გაწრფივებული ამოცანისადმი ასეთი მიდგომით მიღებული ამონახსნი იგივეა, რაც მხები მატრიცის მეთოდით მიღებული, რომელიც თავის მხრივ არაწრფივი სასრული ელემენტის ანალიზის მნიშვნელოვანი ინგრედიენტია. მიღებული შედეგი საშუალებას იძლევა ანალიზურად შემოწმდეს ჰიპოთეზები გვერდით გრეხვაზე დამატებითი პირობების არსებობის შემთხვევაში.

REFERENCES

1. *H.A. Mang, X. Jia, G. Höfinger* (2012), Finite Element Analysis of Buckling of Structures at Special Prebuckling States. Journal of Theoretical and Applied Mechanics, in print.
2. *H.A. Mang, G. Höfinger* (2012), Bifurcation Buckling from a Membrane Stress State. International Journal for Numerical Methods in Engineering, in print.
3. *P. Helnwein* (1997), Zur initialen Abschätzbarkeit von Stabilitätsgrenzen auf nicht- linearen Last-Verschiebungspfaden elastischer Strukturen mittels der Methode der Finiten Elemente. Ph.D. Thesis, Vienna University of Technology, Vienna, Austria.
4. *M. Aminbaghai, W. Pilgram* (1999), Praktische Anwendungsbeispiele für die analytische Lösung linearer Differentialgleichungen mit veränderlichen Koeffizienten. Bauinformatik Journal, 6/1999, pp. 17- 24.
5. *C. Petersen* (1980), Statik und Stabilität der Baukonstruktionen, Friedr. Vieweg & Sohn, Braunschweig/ Wiesbaden.
6. *K. Schneider, H. Rubin* (2008), Schneider Bautabellen für Ingenieure. Bautabellenbuch, 18th Edition.
7. *O.C. Zienkiewicz, R.L. Taylor* (1989),The Finite Element Method 2: Solid and Fluid Mechanics, Dynamics, and Non-Linearity, McGraw-Hill, 4th Edition.
8. *M. Schneider-Bürger* (2001), Stahlbau-Profile, Verlag Stahleisen GmbH, Düsseldorf, 23thEdition.

Received February, 2012